

Longitudinal relaxation and thermoactivation of quantum superparamagnets

D. Zueco and J. L. García-Palacios

*Departamento de Física de la Materia Condensada e Instituto de Ciencia de Materiales de Aragón
C.S.I.C -Universidad de Zaragoza, E-50009 Zaragoza, Spain*

(Dated: November 14, 2018)

The relaxation mechanisms of a quantum nanomagnet are discussed in the frame of linear response theory. We use a spin Hamiltonian with a uniaxial potential barrier plus a Zeeman term. The spin, having arbitrary S , is coupled to a bosonic environment. From the eigenstructure of the relaxation matrix, we identify two main mechanisms, namely, thermal activation over the barrier, with a time scale Λ_1^{-1} , and a faster dynamics inside the potential wells, with characteristic time Λ_w^{-1} . This allows to introduce a simple analytical formula for the response, which agrees well with the exact numerical results, and cover experiments even under moderate to strong fields in the superparamagnetic range. In passing, we generalize known classical results for a number of quantities (e.g., integral relaxation times, initial decay time, Kramers rate), results that are recovered in the limit $S \rightarrow \infty$.

PACS numbers: 03.65.Yz, 05.40.-a, 75.50.Xx, 75.50.Tt

I. INTRODUCTION

Superparamagnets are nanoscale magnetic solids or clusters effectively described in terms of their net spin. They have an internal anisotropy barrier and several local equilibrium states. The spin is coupled to the environmental degrees of freedom of the host material (phonons, nuclear spins, electrons, . . .). This coupling provokes disturbances in the spin dynamics producing jumps over the barrier, thus magnetization reversals, giving rise to the phenomenon of *superparamagnetism*. The prefix *super* stands for the typically large net spins of these systems ($S \sim 10^1$ – 10^4).

Single-domain magnetic particles are an example of such nanoscale solids, having a magnetic moment of a few thousand Bohr magnetons [1]. Due to their enormous spin these particles can be described classically [2, 3]. Another example is provided by single-molecule magnets, such as Mn_{12} , Fe_8 , or Ni_{12} [4]. Their net spin is $S \sim 10$, so that the classical description is no longer valid, and a quantum treatment is required. Still, these molecules comprise some hundreds of atoms, yielding an interplay of quantumness and mesoscopicity that has stimulated an active research in recent years.

Classically, the spin surmounts the barrier ΔU by thermal activation. When $\Delta U/k_B T \gg 1$ the characteristic time for the overbarrier process can be approximately written in the Arrhenius form $\tau \equiv \Lambda_1^{-1} \propto \exp(\Delta U/k_B T)$. This is the rotational counterpart of the Kramers' rate in the theory of activated processes in translational systems [5, 6]. The classical dynamics of these systems has been studied extensively. In particular, the analysis of *longitudinal* response revealed that the one-mode relaxation picture with a characteristic time Λ_1^{-1} is not valid in general [7, 8]. A satisfactory description, however, is provided by a two mode response, one mode corresponding to the overbarrier flux and the other, with a time scale Λ_w^{-1} , describing the faster intrawell dynamics [9].

Quantum mechanically, the spin reversal can take place by thermal activation or tunneling (or a combination

of both) [10, 11, 12, 13]. Tunneling occurs from one side of the barrier to the other (Fig. 1) between resonant states “coupled” by transverse fields (or high-order anisotropy terms). However in the superparamagnetic regime ($T \geq 2$ K) thermal activation controls the physics: out-of-resonance, the crossings are only driven by thermal activation, while tunneling in resonance has the effect of lowering the barrier a few states.

The theory of quantum thermal activation has focused mainly on the zero, or very small bias limit [14, 15]. Then the relaxation becomes well described by one mode, the overbarrier process. The effect of bias fields has been only studied on the thermoactivation rate [16], but not on the susceptibility, beyond the weak-field regime. Thus studies of the full dynamical response including the effect of external fields are demanded. This is the issue we address in this work: the relaxation of a spin with arbitrary S in contact with a bosonic (phonon) environment. The dynamics is studied in the frame of quantum master (balance) equations. We concentrate on the case of longitudinal applied fields, giving a complete characterization of the relaxation mechanisms. The discreteness of the levels plays an important role in some aspects of the dynamics. The connection with the classical theory is done taking the $S \rightarrow \infty$ limit (whenever well defined) recovering known classical results.

The paper is organized as follows. In Sec. II we present the quantum balance equations. The tools of linear-response theory employed and the eigenstructure of the relaxation matrix are discussed in Sec. III. The relaxation eigenvalue spectrum suggest the introduction of a two-mode description of the susceptibility (Sec. IV) following closely the approach of Kalmykov and co-workers in the classical limit [9, 17]. The comparison between exact numerical results and such analytical approximation is done in Sec. V. We also give a complete characterization of the response and simplified expressions (both for the susceptibility and relaxation times) in the range $\Delta U/k_B T \sim 10$ – 20 , experimentally the most relevant for superparamagnets. Technical details for some calcula-

tions are sent to the appendices.

II. QUANTUM SPIN IN A BOSONIC BATH

A. Spin Hamiltonian

The minimal Hamiltonian capturing the physics of superparamagnets includes a uniaxial anisotropy term plus the Zeeman coupling with external fields. Here we study the longitudinal relaxation. Thus only fields parallel to the anisotropy axis will be considered:

$$\mathcal{H} = -DS_z^2 - B_z S_z. \quad (1)$$

In the standard basis $|m\rangle$ this Hamiltonian provides a spectrum ϵ_m with a double well structure with minima at $m = \pm S$ (for $B_z < D(2S - 1)$; see Fig. 1). The barrier heights are $\Delta U_{\pm} = \epsilon_{m_b} - \epsilon_{\pm S}$, where m_b is the index corresponding to the maximum level [18]. For fields $B_z \geq D(2S - 1)$ the barrier disappears.

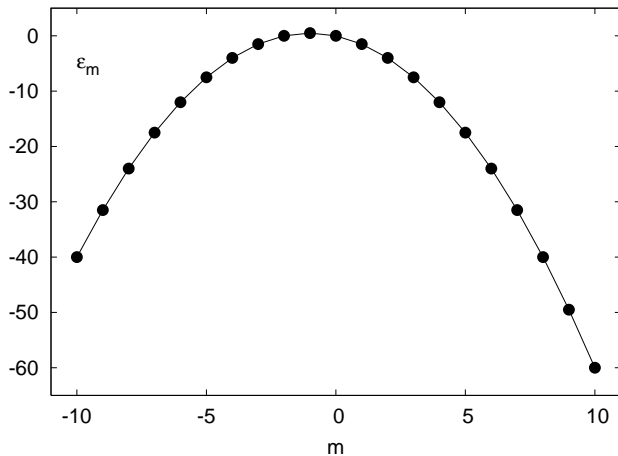


FIG. 1: Energy levels for a spin $S = 10$ described by the Hamiltonian (1) with $D = 0.5$ at $B_z = 1$. Considering that D is given in Kelvin, the value used is closed to Mn_{12} .

B. Balance equations

In contact with a bath, the dynamical equation for the diagonal terms of the density matrix ρ typically has a balance-equation form [16, 19, 20]:

$$\dot{N}_m = (P_{m|m+1}N_{m+1} - P_{m+1|m}N_m) + (P_{m|m-1}N_{m-1} - P_{m-1|m}N_m), \quad (2)$$

where $N_m \equiv \rho_{mm} = \langle m|\rho|m\rangle$. The transition probabilities $P_{m|m'}$ depend on the energy differences $\Delta_{mm'} \equiv \epsilon_m - \epsilon_{m'}$. They fulfill the detailed balance condition:

$$P_{m|m'} = e^{-\beta\Delta_{mm'}} P_{m'|m}, \quad (3)$$

which ensures that the Gibbs distribution, $N_m^{(0)} = e^{-\beta\mathcal{H}(m)}/\mathcal{Z}$, would be a stationary solution of (2) ($\dot{N}_m = 0$). The balance equations can be obtained in a phenomenological way: postulating the form (2) and then calculating the probabilities $P_{m|m'}$ by means of Fermi's golden rule [14].

Equation (2) is a set of linear differential equations. In matrix form it can be written as $\dot{\mathbf{N}} = -\mathcal{R}\mathbf{N}$, with $[\mathbf{N}]_m \equiv N_m$ and \mathcal{R} the relaxation matrix. We assume \mathcal{R} diagonalizable, and write the solution for N_m as:

$$\mathbf{N} = \sum_{i=1}^{2S} c_i e^{-\Lambda_i t} |\Lambda_i\rangle + |\Lambda_0\rangle \quad (4)$$

with Λ_i the eigenvalues of \mathcal{R} and $|\Lambda_i\rangle$ the associated eigenvectors. The last term in (4) corresponds to the equilibrium solution, i.e., $|\Lambda_0\rangle_m \equiv N_m^{(0)}$. The relaxation matrix \mathcal{R} must give $\text{Re}(\Lambda_i) > 0$, ensuring that the asymptotic solution will be the equilibrium one [20].

C. Spin plus bath formulation

Apart from phenomenologically, the balance equations (2) can be obtained in a more rigorous way [10, 16, 20]. One starts from a total Hamiltonian representing the spin plus its environment:

$$\mathcal{H}_{\text{tot}} = \mathcal{H}(\mathbf{S}) + \sum_{\mathbf{q}} V_{\mathbf{q}} F_{\mathbf{q}}(\mathbf{S})(a_{\mathbf{q}}^{\dagger} + a_{-\mathbf{q}}) + \mathcal{H}_{\text{B}}. \quad (5)$$

Here $\mathcal{H}_{\text{B}} = \sum_{\mathbf{q}} \omega_{\mathbf{q}} a_{\mathbf{q}}^{\dagger} a_{-\mathbf{q}}$ is a bosonic bath modelling the host material, the $F_{\mathbf{q}}(\mathbf{S})$ the spin-dependent part of the interaction, and $V_{\mathbf{q}}$ coupling constants. If the spin-bath coupling is weak, the equation of motion for the density matrix ρ can be obtained within perturbation theory. In absence of transverse fields, the diagonal elements of the equation for ρ form a closed set of kinetic equations like (2), with transition probabilities

$$P_{m|m'} = |L_{m,m'}|^2 W_{m|m'}. \quad (6)$$

The $L_{m,m'}$ are matrix elements of the spin-dependent part of the coupling $F(\mathbf{S})$ and the rates $W_{m|m'} \equiv W(\Delta_{mm'})$, are given in terms of the following universal function [19]

$$W(\Delta) = \frac{\lambda \Delta^{\kappa}}{e^{\beta\Delta} - 1}. \quad (7)$$

Here we have considered that the spectral density of the bath, $J(\omega) = \frac{\pi}{2} \sum_{\mathbf{q}} |V_{\mathbf{q}}|^2 \delta(\omega - \omega_{\mathbf{q}})$, has the form $J(\omega) \propto \omega^{\kappa}$ at low ω . When $\kappa = 1$ the bath is called *Ohmic*, while if $\kappa > 1$ it is called *super-Ohmic*.

Having molecular magnets in mind, we will use the following coupling [10, 12]: $F(\mathbf{S}) \propto \{S_z, S_{\pm}\}$, then $L_{m,m\pm 1} = (2m \pm 1) \sqrt{S(S+1) - m(m \pm 1)}$ [19]. In addition the bath will be super-Ohmic ($\kappa = 3$). This models

the interaction with 3D phonons considering one-phonon emission and absorption process, the relevant ones at low temperatures for single-molecule magnets. The modifications required to include other structures of the coupling, or other baths, would only involve the $P_{m|m'}$ and they are easy to carry out.

D. Classical limit

As we would like to make the connection of our results with known classical results, let us briefly consider the $S \rightarrow \infty$ limit of the balance equations (2). To this end it is useful to introduce the scaled quantities:

$$\sigma \equiv \beta D S^2, \quad \xi \equiv \beta B_z S, \quad h \equiv \frac{\xi}{(2 - \frac{1}{S})\sigma}. \quad (8)$$

In terms of them the scaled Hamiltonian reads $\beta\mathcal{H} = -\sigma(m/S)^2 - \xi(m/S)$. The first two quantities are equivalent to those used in the description of classical magnetic nanoparticles. The ‘‘reduced field’’ h , is B_z measured in terms of the field for barrier disappearance $D(2S - 1)$; it differs from the usual classical definition $h_{cl} = \xi/(2\sigma)$, as a consequence of the discreteness of the energy levels.

The quantities σ and ξ should be kept constant when taking the limit $S \rightarrow \infty$. Then $h \rightarrow h_{cl}$ and $\beta\mathcal{H} \rightarrow -\sigma z^2 - \xi z \equiv u(z)$. Physically more and more levels are introduced, towards a continuum, while keeping the anisotropy barrier and Zeeman energy constant. In this limit the transition frequencies $\Delta_{m,m\pm 1}$ tend to zero. Thus, no relaxation is left in the classical case if $P_{m|m\pm 1}(0) = 0$ (see App. A). Such is the case for a pure super-Ohmic environment. A well defined classical limit ($P_{m|m\pm 1}(0) \neq 0$) is obtained considering an *Ohmic* bath. For instance, for coupling to electron-hole excitations or just adding two phonon processes (Raman scattering) in the interaction to phonons. In those cases, the balance equation (2) goes in the limit $S \rightarrow \infty$ over a partial differential (*Fokker-Planck*) equation:

$$\frac{\partial W}{\partial t} = \frac{\partial}{\partial z} \left[D(z) \left(\frac{\partial W}{\partial z} + \frac{\partial u}{\partial z} W \right) \right], \quad (9)$$

with $W(z, t)$ the probability distribution of z ($\sim m/S$) and $P_{m+1|m}(0)/S^2 \rightarrow D(z)$ (see App. A for the details).

III. ANALYSIS OF THE LONGITUDINAL RESPONSE

The purpose of this section is to present the theoretical tools necessary to describe the relaxation of a spin S . To made a system to ‘‘relax’’ we must put it in a non-equilibrium situation (e.g., subjecting it to a perturbation in the external field). The response to this probe informs about the relaxation mechanisms of the system. We will use linear-response-theory tools [21] and the analysis of the eigenstructure of the relaxation matrix.

A. Linear response theory

For the effect of the applied perturbation to reflect the intrinsic properties of the system the force should be suitable small. The weakness of the probe has the technical advantage of allowing the use of linear response theory. Several ‘‘experiments’’ can be made to study the response, namely, subjecting it to a sudden constant ‘‘force’’ or by removing the force after having kept it on for a long time. One can also consider the response to a force oscillating with frequency Ω . Linear response theory provides an intimate relationship between these types of measurements.

Assume first that we have excited the system with a constant field δB_z , keeping it on until the system is equilibrated (in a total field $B_z^0 + \delta B_z$). Then, we switch the perturbation off and measure the response:

$$\Delta M_z(t) \equiv \langle M_z(t) \rangle - \langle M_z \rangle_0, \quad (10)$$

with $\langle M_z \rangle_0$ the statistical average at equilibrium with $B_z = B_z^0$ and $\langle M_z(t) \rangle = \sum_{m=-S}^S m N_m(t)$. Since the asymptotic solution for \mathbf{N} is the equilibrium one in $B_z = B_z^0$ then $\langle M_z \rangle_0 = \langle M_z(t \rightarrow \infty) \rangle$. Next, introducing the solution (4) for $N_m(t)$ in $\langle M_z(t) \rangle$, we find

$$\Delta M_z = \chi_z \delta B_z \sum_{i=1}^{2S} a_i e^{-\Lambda_i t} \quad (11)$$

where χ_z is the equilibrium susceptibility: $\chi_z \equiv \partial \langle M_z \rangle_0 / \partial B_z$. In linear response χ_z is equal to $[\langle M_z(0) \rangle - \langle M_z(\infty) \rangle] / \delta B_z$. The coefficients a_i are given in terms of the eigenvalues of the relaxation matrix \mathcal{R} and the coefficients c_i by [see Eq. (4)]:

$$a_i = \frac{1}{\chi_z} \tilde{c}_i \sum_{m=-S}^S m |\Lambda_i \rangle_m. \quad (12)$$

Here c_i has been redefined as $\tilde{c}_i \equiv c_i / \delta B_z$, to get rid of dependences on δB_z . The coefficients a_i obey the normalization condition: $\sum_{i=1}^{2S} a_i = 1$ which follows from the definition (12) and the equality: $\chi_z = \sum_i \tilde{c}_i \sum_m m |\Lambda_i \rangle_m$. The \tilde{c}_i can be evaluated making $t = 0$ in Eq. (4). The initial condition is the system equilibrated at $B = B_z^0 + \delta B_z$. The occupation numbers can be written in linear approximation as $N_m(t = 0) \cong N_m^{(0)} B_z^{(0)} + \delta B_z \partial_{B_z} N_m^{(0)}|_{B_z^0}$, so that the \tilde{c}_i 's obey

$$\frac{\partial N_m^{\text{eq}}}{\partial B_z} \Big|_{B_z^0} = \sum_{i=1}^{2S} \tilde{c}_i |\Lambda_i \rangle_m, \quad (13)$$

which is an overdetermined set of $2S + 1$ linear equations (there are $2S$ c_i 's). Both $|\Lambda_1 \rangle$ and \tilde{c}_i can be obtained using standard numerical routines [22].

Finally, let us consider the relation with the other relaxation experiments. The case with the system equilibrated at $B_z = B_z^0$ and a perturbation δB_z suddenly

added is just the complementary situation to case discussed above. More interesting is the oscillating field probe. Here we define the dynamical susceptibility, $\chi(\Omega)$, as the coefficient which relates (in the frequency domain) response and excitation: $\Delta\widetilde{M}_z(\Omega) = \chi(\Omega)\delta\widetilde{B}_z(\Omega)$ with $\widetilde{g}(\Omega) = \int dt e^{-i\Omega t}g(t)$. Then the response to a periodic perturbation $\delta B_z(t) \propto e^{-i\Omega t}$ is given by

$$\begin{aligned}\chi(\Omega) &= \chi_z \left[1 - i\Omega \int_0^\infty dt \frac{\Delta M_z(t)}{\Delta M_z(0)} e^{-i\Omega t} \right] \\ &= \chi_z \sum_{i=1}^{2S} \frac{a_i}{1 + i\Omega\Lambda_i^{-1}}\end{aligned}\quad (14)$$

Equations (11) and (14) provide the relation between the different relaxation experiments. The analysis of the response gives the time scales Λ_i^{-1} and the weights a_i 's of the modes involved in the relaxation process. To conclude, note that neither Λ_i nor a_i depend on the external probe but only on the intrinsic dynamics of the system, as it was demanded.

B. Eigenvalue and eigenvector structure

Attending at the evolution of \mathbf{N} in Eq. (4), we see that the eigenvalues of \mathcal{R} give the different time scales Λ_i^{-1} in the relaxation, while the eigenvectors provide the change in the population levels. The eigenvalues and eigenvectors for $S = 10$, obtained by numerical diagonalization of \mathcal{R} , are plotted in Figs. 2 and 3.

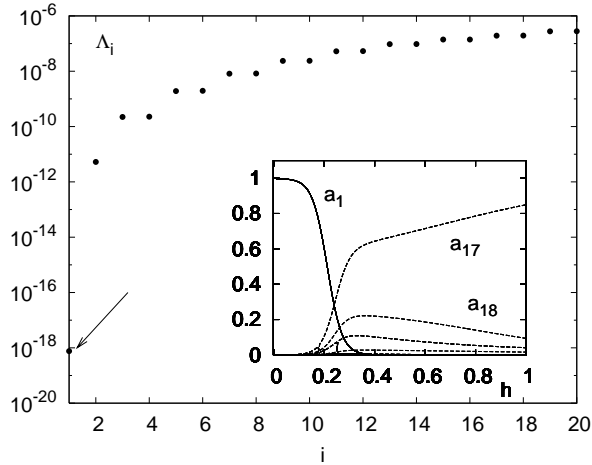


FIG. 2: Eigenvalues of the relaxation matrix for $S = 10$. The spin-bath coupling is $\lambda = 10^{-9}$, $\sigma = \beta DS^2 = 15$ and $h = 10^{-3}$. The arrow marks the lowest non-vanishing eigenvalue Λ_1 . Inset: coefficients a_i as a function of h for the same S , λ , and σ .

Apart from the zero eigenvalue (not plotted in Fig. 2), the eigenvalues correspond to two, well separated, sets of time scales. From the structure of the eigenvectors (Fig. 3) we see that the dynamics induced by $|\Lambda_1\rangle$ produces the increment in the population in one well and

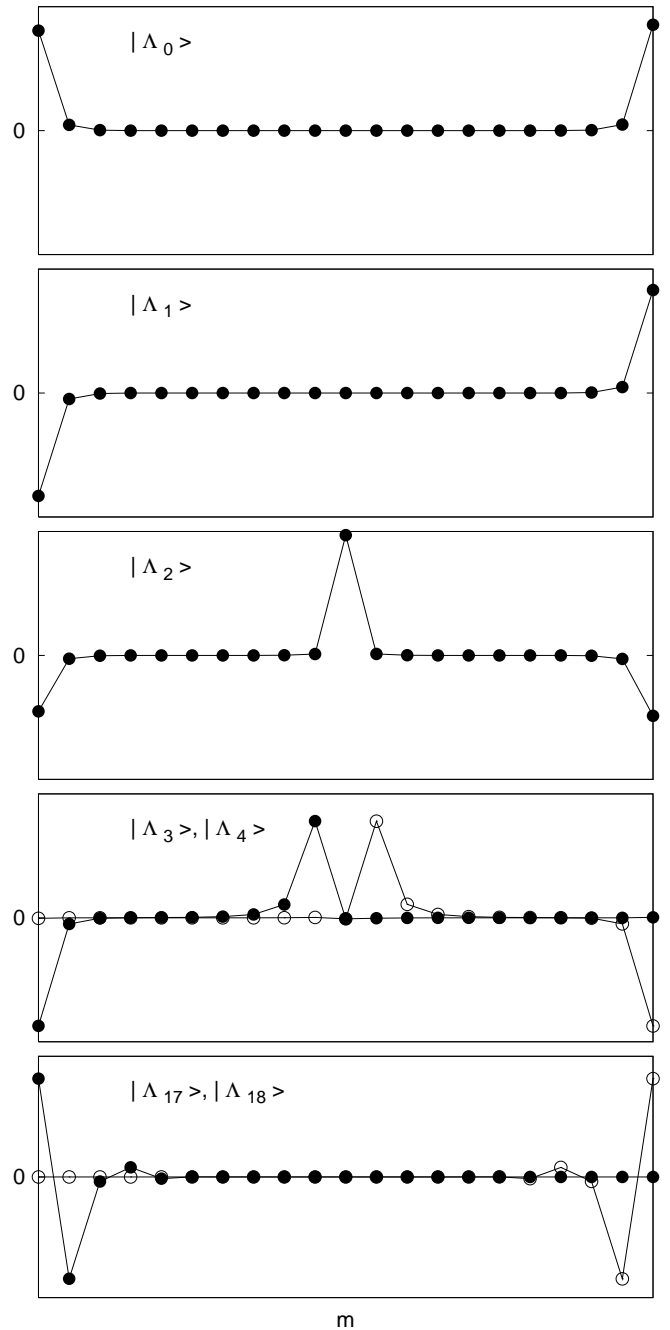


FIG. 3: Eigenvectors of the relaxation matrix for $S = 10$, $\sigma = 15$, $h = 10^{-3}$ and $\lambda = 10^{-9}$. At $h = 0$ the states Λ_{2m-1} and Λ_{2m} ($m \geq 2$) are degenerated. Numerical diagonalization gives even-odd eigenvectors, so we use a small $h = 10^{-3}$.

the depopulation of the other. Since this transfer occurs across the barrier, $|\Lambda_1\rangle$ is associated to the overbarrier dynamics. On the other hand, $|\Lambda_2\rangle$ represents the transfer from $m = 0$ to both wells or viceversa. Further, $|\Lambda_3\rangle$ and $|\Lambda_4\rangle$ account for dynamics involving $m = \pm 1$ and $m = \pm S$ respectively, and so on. Eventually $|\Lambda_{17}\rangle$ – $|\Lambda_{20=2S}\rangle$, involve the levels close the bottom of the wells. All these processes are called intrawell ones, since no

activation over the barrier is required. Thus the slow, and well separated, time scale Λ_1^{-1} corresponds to the overbarrier dynamics, whereas the set of (comparatively close) intrawell processes is responsible for the fast dynamics.

Let us briefly comment on two aspects of the eigenstructure. First, apart from Λ_0 , Λ_1 and Λ_2 , the remaining eigenvalues appear doubly degenerated (at $h = 0$) [23]. Physically each member of the degenerate pair describes identical processes in different wells, and at $B_z = 0$ both wells are equivalent. When $B_z \neq 0$ the equivalence is broken and the degeneration lifted.

Finally a connection with the classical case can be sketched. The *Fokker-Planck* limit (9) of the balance equations (2) defines a Sturm-Liouville problem. From the corresponding theory we know that the eigenvalues of the differential operator are real and we can order them: $\Lambda_0^{\text{cl}} \leq \Lambda_1^{\text{cl}} \leq \Lambda_2^{\text{cl}} \leq \dots$. Their corresponding eigenvectors $|\Lambda_n^{\text{cl}}\rangle$ have n nodes. Restricting ourselves to $h = 0$, the problem is invariant under the transformation $z \rightarrow -z$. Then there exists a basis where the states are even or odd under $z \rightarrow -z$. Then $|\Lambda_0^{\text{cl}}\rangle$ (the Gibbs solution) is an even function with zero nodes. Next $|\Lambda_1^{\text{cl}}\rangle$, would be an odd function since it has 1 node, $|\Lambda_2^{\text{cl}}\rangle$ an even function (with 2 nodes), and so on. These features are retained in the discrete ($S < \infty$) case (Fig. 3). Actually, from the degenerate states (e.g., $|\Lambda_3\rangle$ and $|\Lambda_4\rangle$) we can form the symmetrical and antisymmetrical combinations $|\Lambda_3\rangle \pm |\Lambda_4\rangle$, fully recovering the even-odd picture.

IV. ANALYTICAL APPROACH

In general, the response will depend on $2S$ modes [see Eqs. (11) and (14)]. However, taking into account the eigenvalue structure of the previous section, we approximate the response in terms of two main processes (see Sec. III B). One accounting for the overbarrier dynamics, with characteristic time Λ_1^{-1} , and the other describing the intrawell dynamics with a time scale Λ_w^{-1} . The latter is a kind of *collective* mode which describes the close set of intrawell processes. This motivation for the two-mode approximation is reinforced by the good results it yields in the classical limit [9, 17].

A. Bimodal approximation

Suppose that the relaxation can be approximated by two exponentials:

$$\Delta M_z(t) \cong \chi_z \delta B_z [a e^{-\Lambda_1 t} + (1-a) e^{-\Lambda_w t}], \quad (15)$$

or, in the frequency domain,

$$\frac{\chi(\Omega)}{\chi_z} \cong \frac{a}{1 + i\Omega\Lambda_1^{-1}} + \frac{(1-a)}{1 + i\Omega\Lambda_w^{-1}}. \quad (16)$$

Note first that this bimodal description is exact for $S = 1$ (see App. D). In general a and Λ_w are coefficients to be

identified with known magnitudes of the problem. This can be carried out following the approach of Kalmykov and co-workers in the classical case [9]. They observed that we have two unknown parameters (a and Λ_w), while $\chi(\Omega)$ can be evaluated in two extreme limits, namely, the low- Ω and high- Ω ranges. Then, taking these limits in the above two mode approximation, a and Λ_w are identified.

The low frequency behavior of $\chi(\Omega)$ is given by:

$$\chi(\Omega) \cong \chi_z (1 - i\Omega\tau_{\text{int}} + \dots), \quad (17)$$

with τ_{int} the integral relaxation time, defined as the area under the magnetization relaxation curve after a sudden change δB_z at $t = 0$:

$$\tau_{\text{int}} \equiv \int_0^\infty dt \frac{\Delta M_z(t)}{\Delta M_z(0)}. \quad (18)$$

Next, in the high- Ω limit the susceptibility can be expanded as:

$$\chi(\Omega) \cong \chi_z \frac{i}{\Omega\tau_{\text{ef}}}, \quad \tau_{\text{ef}}^{-1} \equiv \left. \frac{d}{dt} \left(\frac{\Delta M_z(t)}{\Delta M_z(0)} \right) \right|_{t=0}, \quad (19)$$

where τ_{ef} is the initial slope of the relaxation.

The proposed formula (16) must obey the exact asymptotic equations (17) and (19), whence:

$$\tau_{\text{int}} = a/\Lambda_1 + (1-a)/\Lambda_w \quad (20)$$

$$\tau_{\text{ef}}^{-1} = a\Lambda_1 + (1-a)\Lambda_w, \quad (21)$$

These equations can be solved for a and Λ_w , yielding:

$$a = \frac{\tau_{\text{int}}\tau_{\text{ef}}^{-1} - 1}{\Lambda_1\tau_{\text{int}} - 2 + (\Lambda_1\tau_{\text{ef}})^{-1}} \quad (22)$$

$$\Lambda_w = \frac{\Lambda_1 - \tau_{\text{ef}}^{-1}}{\Lambda_1\tau_{\text{int}} - 1} \quad (23)$$

This reduces the problem to the obtainment of the three characteristic times Λ_1^{-1} , τ_{int} , and τ_{ef} . Naturally, they can be expressed in terms of the relaxation eigenvalues:

$$\tau_{\text{int}} = \sum_i \frac{a_i}{\Lambda_i}, \quad \tau_{\text{ef}}^{-1} = \sum_i a_i \Lambda_i. \quad (24)$$

However, the goal is to bypass the eigenvalue computation by calculating them directly.

B. Calculation of τ_{int} , Λ_1 and τ_{ef}

In the classical limit, Brown [3] calculated the lowest eigenvalue Λ_1 in the high barrier case (see also [24]). Besides Coffey and co-workers derived τ_{ef} [25]. On the other hand, Garanin calculated τ_{int} for a system of balance equations to which Eq. (2) can be reduced. In this subsection we are going to extend the results for Λ_1 and τ_{ef} to the quantum case (recovering the classical results in the limit $S \rightarrow \infty$), and that of τ_{int} to the generic system (2) of balance equations. This will result in a closed expression for the bimodal formula (16).

1. Integral relaxation time, τ_{int}

The calculation of τ_{int} is based in that the susceptibility can be calculated analytically up to first order in Ω [16]. Exploiting this fact, one finds for τ_{int} (see App. B):

$$\tau_{\text{int}} = \frac{\beta}{\chi_z} \sum_{m=-S}^S \frac{\Phi_m^2}{N_m^{(0)} P_{m+1|m}} \quad (25)$$

where

$$\Phi_m = \sum_{j=-S}^m (M_z - j) N_j^{(0)}. \quad (26)$$

Notice that Φ_m only involves equilibrium averages, being independent of the spin-bath coupling model.

The dependence of $P_{m|m'}$ in the denominator on the energy differences, gives *minima* at the crossing fields [26], which remind of the *maxima* in the relaxation rate due to tunneling.

2. Lowest eigenvalue Λ_1

The calculation of Λ_1 , which corresponds to the Kramers rate, constitutes an important task by itself. Needless to say its relevance in the theory of activated processes [5, 6]. In the classical case it is possible to derive an expression for Λ_1 [3], giving good results for not too strong fields [24]. In the quantum case, a closed analytical expression for Λ_1 exists only for $h = 0$ due to Villain and co-workers [14] and later on reexamined and improved by Würger [15]. Their result can be written in a form appropriate for future comparison as:

$$\Lambda_1^{-1} = \sum_{m=0}^{S-1} \frac{\theta_m}{N_m^{(0)} P_{m+1|m}} \quad (27)$$

with $\theta_m = \sum_{j=m+1}^S N_j^{(0)}$.

Both Λ_1 from Eq. (27) and τ_{int}^{-1} , together with the exact numerical Λ_1 are displayed in Fig. 4 showing their agreement at $h = 0$. However, as we increment the field τ_{int}^{-1} and Λ_1 deviate from each other. This is natural, should $\tau_{\text{int}}^{-1} \cong \Lambda_1$, the response would be described by one mode, namely the overbarrier [i.e., $a \cong 1$ in the bimodal approximation, see Eq. (20)]. The same behavior was found in the classical limit [7, 8]. The physical reason for the disagreement between τ_{int}^{-1} and Λ_1 is the intrawell processes entering into scene at finite h . Formally, at $h \ll 1$, the quantity $\Phi_m^2 / P_{m+1|m} N_m^{(0)}$ is highly peaked at the barrier ($m = m_b$), and well approximated by the overbarrier process; then $\tau_{\text{int}}^{-1} \cong \Lambda_1$. Increasing the field, however, Φ_m^2 develops a second peak around the bottom of the lower well, $m \cong S - 1$, and the sum acquires a relevant contribution from the intrawell processes [8] (see also Fig. 8).

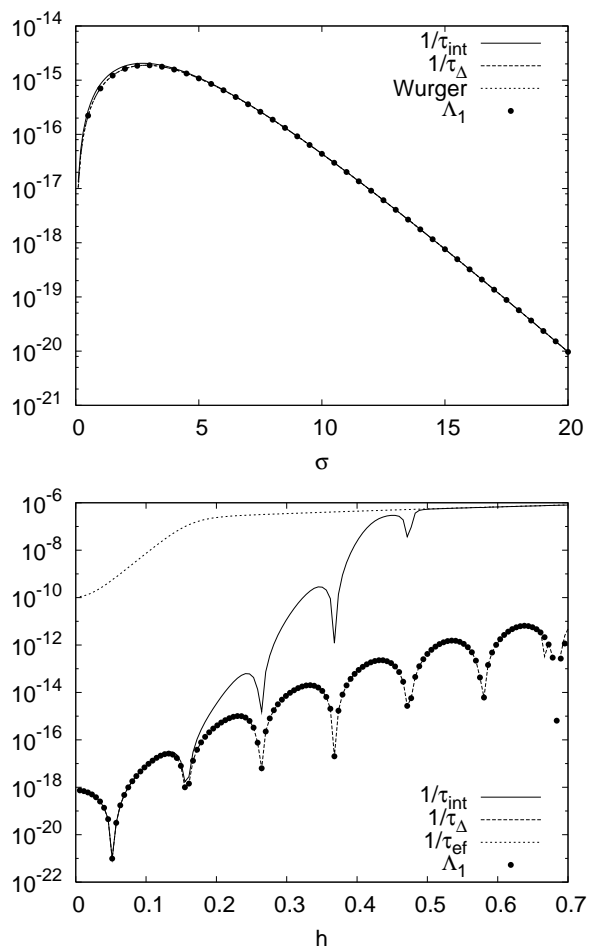


FIG. 4: Top: Comparison between the analytical τ_{int}^{-1} [Eq. (25)], τ_{Δ}^{-1} [Eq. (27)] and the numerical lowest eigenvalue Λ_1 in the unbiased case as a function of σ , the barrier height. The parameters are $S = 10$, $T = 0.1$ and $\lambda = 10^{-9}$. Würger's result and τ_{Δ} have a maximum relative deviation of 10^{-3} in the plotted range (at the lowest barrier heights). Bottom: τ_{int}^{-1} , τ_{Δ}^{-1} , τ_{ef}^{-1} [Eq. (32)] and Λ_1 for $S = 10$, $\lambda = 10^{-9}$ and $\sigma = 15$ as a function of the field. The relative difference between τ_{int}^{-1} and Λ_1 never exceeds the 1% at not too strong fields ($h \leq 0.5$). For $h \geq 0.7$ we find numerical instabilities at these values of σ and S .

To generalise the calculation of Λ_1 , we need an observable where only overbarrier processes are reflected. Then its associated integral relaxation time would probably be well approximated by Λ_1 . This can be done generalizing to the quantum case the new integral relaxation time, τ_{Δ} , introduced by Garanin for the classical Fokker-Planck equation [27]. To this end, one chooses as observable the difference of the well populations $\Delta \equiv N_+ - N_-$. To obtain the integral relaxation time associated to Δ , we need its low- Ω behavior, involving the “static” response $\chi_{\Delta} \sim \partial_{B_z} \Delta$ [cf. the case of the magnetization (17)]:

$$\chi_{\Delta}(\Omega) = \frac{\partial \Delta(\Omega)}{\partial B_z} \cong \chi_{\Delta}(1 + i\Omega\tau_{\Delta} + \dots). \quad (28)$$

This is done in App. B, yielding the following τ_Δ

$$\tau_\Delta = \frac{\beta}{\chi_\Delta} \sum_{m=-S}^{S-1} \frac{\Phi_m \Phi_m^N}{N_m^{(0)} P_{m+1|m}} \quad (29)$$

with (m_b is the maximum level)

$$\Phi_m^N = \sum_{j=-S}^m N_j^{(0)} [\Delta - \text{sgn}(j - m_b)] \quad (30)$$

It results that $\Phi_m \Phi_m^N$ is nearly constant. Then the sum in Eq. (29) has only one main contribution (around the barrier $m \cong m_b$), not reflecting the dynamics inside the wells, as it was intended.

We have seen in Fig. 4 that at $h = 0$, τ_Δ matches Würger result (27) for Λ_1 . In fact, it can be seen that our $\tau_\Delta|_{h=0}$ reduces in the high barrier regime to Eq. (27). (see App. C). Another limit where we have an expression for Λ_1 is the classical one. Taking the limit $S \rightarrow \infty$ in τ_Δ we indeed obtain Brown's result in the high barrier range (App. C)

$$\Lambda_1 \cong \tau_D^{-1} \sigma^{3/2} \pi^{-1/2} (1 - h^2) \left\{ (1 + h) \exp[-\sigma(1 + h)^2] + (1 - h) \exp[-\sigma(1 - h)^2] \right\}. \quad (31)$$

Finally, in the quantum case and $h \neq 0$, we have to check τ_Δ with the numerical results for Λ_1^{-1} ; this was done in Fig. 4 There one sees that, contrary to the ordinary integral relaxation time, τ_Δ^{-1} provides a remarkable approximation for the Kramers' rate.

3. Effective time, τ_{ef}

We conclude with the effective time. By definition τ_{ef} is the initial slope of the magnetization, see Eq. (19). The initial condition is the system at thermal equilibrium with $B_z = B_z^0 + \delta B_z$, so that $N_m(0)$ is known, whence $\dot{N}_m(0)$ follows [directly from Eq. (2)]. Next, $d\Delta M_z/dt|_{t=0}$ is calculated from $\dot{N}_m(0)$ (see App. B for details). This gives the following expression for τ_{ef} :

$$\tau_{\text{ef}}^{-1} = \frac{\beta}{\chi_z} \sum_{m=-S}^S N_m^{(0)} P_{m+1|m}. \quad (32)$$

The classical limit of Eqs. (25), (29) and (32) give the expressions derived over the years from the Fokker-Planck equation (9). They are the sought analytical expressions for the characteristic times τ_{int} , Λ_1^{-1} and τ_{ef} in the quantum case. Together with Eqs. (22) and (23) they provide a closed formula for the response under the bimodal approximation, which can be checked against exact results.

V. ANALYSIS OF THE DYNAMIC RESPONSE

In this section we study the full dynamical response. We compare exact numerical results with the approximate bimodal formula constructed in the previous section. We also present approximate tractable expressions.

A. Exact results vs. bimodal formula

To obtain numerically exact results for the response [see Eqs. (11) and (14)], we compute numerically the eigenvalues Λ_i and the amplitudes a_i [see Eq. (13)]. Comparison between them and the analytical formula (16) is shown in Figs. 5 and 6. In Fig. 5 we plot the field dependence of the susceptibility spectra. The agreement is excellent in the low temperature range (large σ). The

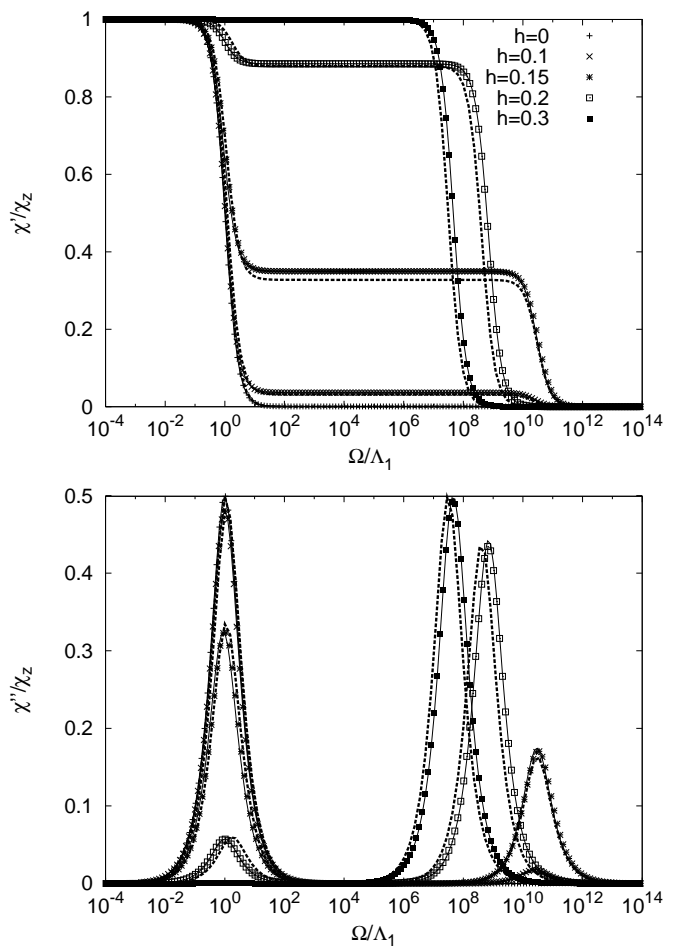


FIG. 5: Real parts (top) and imaginary parts (bottom) of the dynamical susceptibility of a spin $S = 10$ with $\lambda = 10^{-9}$, at $T = 0.1$ and $\sigma = 15$ in various applied fields. The symbols represent the exact numerical results and the solid lines the bimodal formula (16). The dashed (thick) lines correspond to the bimodal formula but with the approximate a , Λ_1 , and Λ_w from Eqs. (34), (35), and (36).

σ -dependence is presented in Fig. 6. The slow dynamics

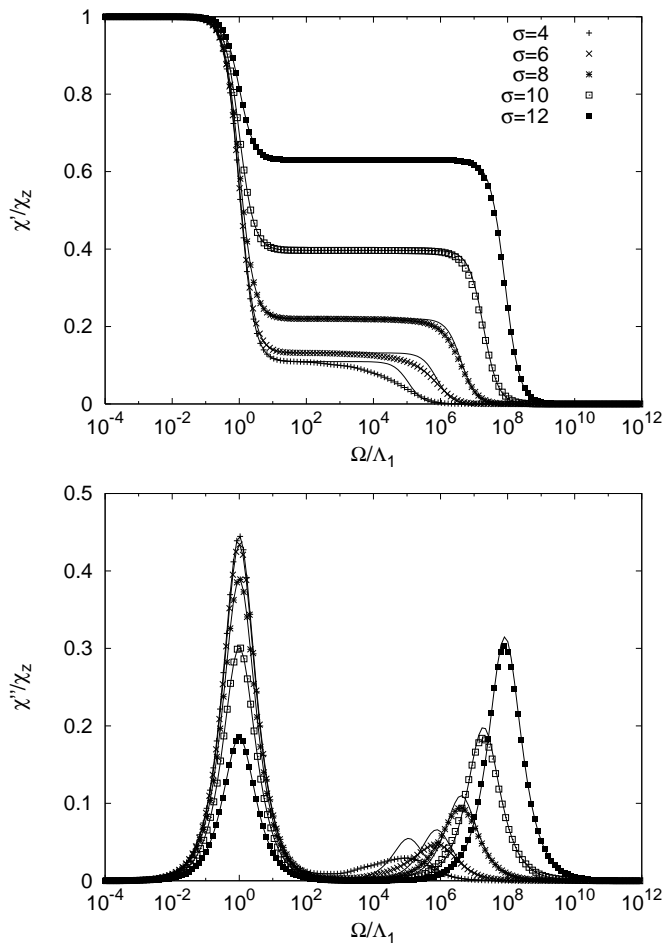


FIG. 6: Real parts (top) and imaginary parts (bottom) of the dynamical susceptibility of a spin $S = 10$ with $\lambda = 10^{-9}$ at $T = 0.1$ and $h = 0.2$. Here $\sigma = 4, 6, 8, 10$ and 12 . Points represent the exact numerical results and lines are the theoretical formula (16).

at $\Omega \sim \Lambda_1$ is well described by the analytical expression, while reducing sufficiently σ the bimodal approximation starts to fail at high frequencies $\Omega \sim \Lambda_w$. Specifically, the second peak in the exact imaginary part is no longer a single Lorentzian and a broadening with respect to the analytical curve is observed.

The reason for the overall agreement between the bimodal approximation and the exact results can be understood as follows. The overbarrier dynamics must be well captured, since it is exactly given by Λ_1 , while Λ_1 is very well approximated by τ_Δ (see Sec. IV). Next, in the two mode approximation we assumed that the intrawell modes are close to one another, so that they can be described with the collective scale Λ_w . We have checked that the degree of closeness does not depend on σ so as to explain the disagreement for low σ and high Ω in Fig. 6. What happens is that at high σ the bimodal approximation works very well because only intrawell processes involving the lowest well states are accessible, yielding $a_i \sim 0$ for the rest of the modes. For the example con-

sidered, $S = 10$, one indeed sees that at $\sigma = 15$, only a_{17} and a_{18} contribute (involving $m = \pm S$ and $m \pm (S - 1)$), and to a smaller extent a_{16} and a_{19} (see the inset in Fig. 2). Lowering enough the barrier more and more intrawell modes play a role yielding a broadening of the curve for the imaginary part of $\chi(\Omega)$. However, we have to go down to $\sigma = 6$ to find large disagreements, while most experiments in these systems involve $\sigma \gtrsim 10-20$.

B. Intrawell versus overbarrier processes

Let us study the relative importance of intrawell and overbarrier dynamics in the response, a subject that received some attention in the classical case [7, 8]. The competition between them becomes mediated by a in our Eq. (16). In particular when $a = 1$ only relaxation across the barrier takes place while at $a = 0$ the opposite occurs. From Fig. 5 and 6, we see that the relative weight of the two modes depends both on h and the barrier height. The field and σ dependence of a is drawn in Fig. 7 for different S . The main features are as follows. Concerning the h dependence, the transition from overbarrier dominated ($a \sim 1$) to intrawell dominated response ($a \sim 0$) is produced in a relatively small window of h . Secondly the transition occurs at larger values of h the smaller the value of S is. In addition, the σ dependence of a shows that the value of S is also crucial in the limit $\sigma \rightarrow \infty$. In this limit a tends to 1 or to 0 depending on S .

Let us try to explain qualitatively these results, invoking a statistical mechanical argument. Inspecting the level structure of the spin Hamiltonian, we see that at $\xi = \sigma/S$ the levels $-m$ and $m - 1$ become degenerated. Such field corresponds to

$$h^* \equiv \frac{1}{2S - 1}. \quad (33)$$

Then, if $h < h^*$ the first excited level is $m = -S$ (in the other well), whereas if $h > h^*$ it is $m = S - 1$ (inside the same well). Approaching the large σ limit we just need to consider the fundamental state and the first excited level. Then, when $\sigma \rightarrow \infty$, if $h < h^*$ intrawell process are inhibited, because only $m = S$ and $m = -S$ are populated, giving $a = 1$. On the contrary if $h > h^*$, the states that contribute are $m = -S$ and $m = S - 1$, in the same well, so that $a = 0$.

The above argument also serves to explain the large σ limits in Fig. 7, because the field used, $h = 0.15$, is lower than $h^*(S = 1, 2, 3)$, and greater than $h^*(S > 3)$. On the other hand, we have $h^* \rightarrow 0$ when $S \rightarrow \infty$. This is in agreement with the classical calculation where $a \rightarrow 0$ as soon as one makes $h \neq 0$ in the limit $\sigma \rightarrow \infty$ [8]. Eventually our statistical mechanical argument also explains the S dependence of the onset of intrawell modes when increasing the field (Fig. 7). Specifically, it gives a step function $\Theta(h^* - h)$ at $\sigma \rightarrow \infty$, while the remaining curves can be understood as a smoothing of the abrupt step due to finite temperature (Fig. 7).

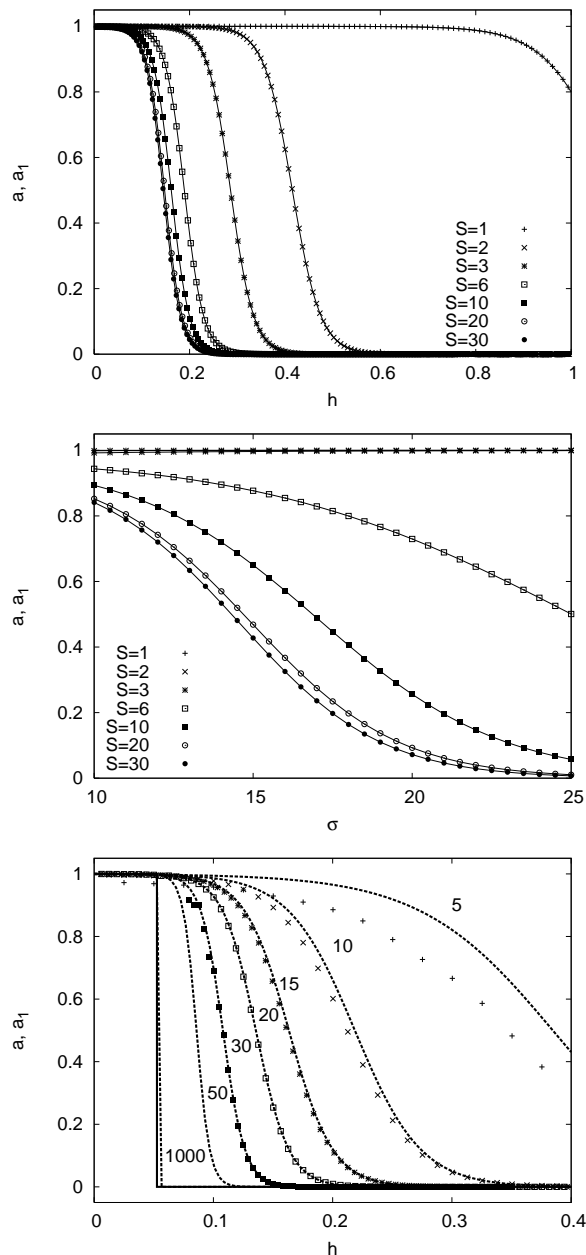


FIG. 7: Top: Field dependence of a_1 (points) and a (lines) for different values of S . We have fixed $\sigma = 15$, $\lambda = 10^{-9}$ and $T = 0.1$. Middle: Barrier dependence of a_1 and a at the same S 's. The effective field has been fixed at $h = 0.15$. Bottom: Field dependence of a_1 and the approximate a of Eq. (34). The numbers stand for the σ value. Increasing σ the curves approach a step function (solid line). At $\sigma = 30$ we find numerical instabilities so that for $\sigma = 50, 1000$ only the approximate formula is plotted.

C. Approximate expressions in the Kramers regime

To conclude we present approximate formulas for the two time scales of the response, Λ_1 and Λ_w , in the high barrier (Kramers) regime, and for the parameter a con-

trolling their relative weight in the response. In this regime a is well described by the formula (see App. C):

$$a \cong \left[1 + \frac{1}{4}(1-q)^2 e^{\sigma(q+1)^2(h-h^*)}\right]^{-1} \quad (34)$$

where $q = (S-1)/S$. Returning for a moment to the previous discussion, note that this formula captures the h , σ and S dependences of Fig. 7; for instance it approaches the step function $\Theta(h - h^*)$ when $\sigma \rightarrow \infty$, and gives its smoothing for finite σ . Note finally that Eq. (34) depends only on parameters of the spin Hamiltonian, being independent of the coupling (as in the classical case [8]).

Let us go now into the Kramers rate. At low temperatures Λ_1 can be expressed in terms of the barriers $\Delta U_{\pm} \equiv \varepsilon_{m_b} - \varepsilon_{\pm S}$ in a clear Arrhenius form (App. C)

$$\Lambda_1 \cong (e^{-\beta\Delta U_+} + e^{-\beta\Delta U_-}) \left(\frac{1}{P_{m_b+1|m_b}} + \frac{1}{P_{m_b-1|m_b}} \right)^{-1}. \quad (35)$$

Recall that the transition probabilities $P_{m|m'} = |L_{m,m'}|^2 W_{m|m'}$ [Eq. (6)], involve the coupling matrix elements $L_{m,m\pm 1} = (2m \pm 1)\sqrt{S(S+1) - m(m \pm 1)}$ and the rates $W_{m|m'} = \lambda \Delta_{m,m'}^{\kappa} / (e^{\beta\Delta_{m,m'}} - 1)$. Equation (35) generalizes the zero-field result of Villain and co-workers [14]. In addition, with the appropriate $L_{m,m\pm 1}$ and the spectral index κ (from $J(\omega) = \lambda \omega^{\kappa}$), it is applicable to other couplings and baths.

Finally we turn to the fastest mode Λ_w . In order to fix some time scale in the problem, we measure Λ_w relative to Λ_1 . Under the same assumptions used to obtain the above a and Λ_1 , we find for Λ_w/Λ_1 :

$$\frac{\Lambda_w}{\Lambda_1} = \frac{1}{4S^2} \frac{a}{1-a} \times \left\{ e^{\beta\Delta U_+} \left[P_{S-1|S} \left(\frac{1}{P_{m_b+1|m_b}} + \frac{1}{P_{m_b-1|m_b}} \right) \right] + e^{\beta\Delta U_-} \left[P_{-S+1|S} \left(\frac{1}{P_{m_b+1|m_b}} + \frac{1}{P_{m_b-1|m_b}} \right) \right] \right\} \quad (36)$$

While the parts involving the barriers ΔU_{\pm} and a , are independent of the coupling model, the transition rates at the wells and at the barrier are quite sensitive to the interaction. Thus the ratio Λ_w/Λ_1 can be used to compare different couplings and baths.

Formulas (34), (35) and (36) provide tractable expressions appropriate for the experiments in the superparamagnetic range, out of resonance conditions (see App. C for further approximate expressions). Their reasonable agreement with the exact numerical results can be seen in Fig. 5. Under resonant conditions, we expect that our equations will still work after some modifications. For example, the barrier height will be lowered, since m_b would not be the barrier top but the state at which the activated tunnel process takes place.

VI. SUMMARY

The relaxation theory of a quantum superparamagnet has been developed. We have studied the minimal model, namely a spin of arbitrary S with uniaxial anisotropy in a longitudinal field. Scarce results were available for the full dynamical response in the presence of external fields. Still, the popular single-Debye form for the susceptibility spectra could be expected to fail, in analogy with the classical situation. Here, these topics have been addressed in the frame of quantum balance equations rigorously grounded on the system-plus-bath approach to quantum dissipative systems.

We began analyzing the eigenstructure of the relaxation matrix associated to the system of balance equations. The form of the eigenvectors allowed us to identify and classify the different relaxation mechanisms. In this way, full content has been given to popular statements about the relation of eigenvalues and relaxation modes. Besides, it has been put in connection with the Sturm–Liouville eigenstructure of the classical Fokker–Planck limit (parity, nodes, etc.).

Two main processes emerge: activation over the anisotropy barrier, with a time scale Λ_1^{-1} , and a bunch of close (in logarithmic scale) fast intrawell modes, with an “average” time scale Λ_w^{-1} . The identification and separation of the modes suggest the introduction of an approximate two-mode expression for the dynamical susceptibility. Then, following the approach of Kalmykov *et al.* for the classical case, the parameters of that formula are expressed in terms of three characteristic quantities: integral relaxation time τ_{int} , lowest non-vanishing eigenvalue Λ_1 (Kramers rate), and the initial slope of the magnetization decay τ_{ef} . The usefulness of the classical approach was that these three times could be obtained analytically (which was done over the years for different relevant situations). Then, we were left with the task of finding them all in analytical form in the quantum domain. This has been accomplished here, getting formulas for the quantum τ_{int} , Λ_1 (via the integral relaxation time for the population difference τ_Δ), and τ_{ef} , which recover known classical results when taking the $S \rightarrow \infty$ limit. With them, one has a bimodal equation for the dynamical susceptibility of a spin with arbitrary S where all ingredients can be expressed in closed form.

We have compared exact numerical results with such bimodal expression; the formula results to be quite accurate, specially in the superparamagnetic regime ($\Delta U/k_B T \sim 10\text{--}20$; the range of major experimental interest). Its limits of validity have been assessed and interpreted in physical terms. Furthermore, in the range where the bimodal description works best, we have derived simple analytical expressions for Λ_1 , Λ_w and a (the parameter controlling the relative weight of the two effective modes). These generalize formulas available at zero field, while they can also be applied to other structures of the coupling and spectral densities of the bath (e.g., Kondo coupling to electron-hole excitations).

In the presence of terms not commuting with S_z in the Hamiltonian (e.g., transverse fields) the situation is expected to be altered by tunnel events between resonant levels $-m$ and $m-k$. Then, the balance equations loose the three-term recurrence form which allowed to derive the closed-form solutions [28]. However, in the superparamagnetic range, thermal activation is still expected to govern the physics. Actually, in non-resonant conditions (the generic case), tunnel is inhibited, while at the resonances, it can be accounted for heuristically by lowering the effective barrier a few states. Thus, we hope that the two-mode picture will be of use with the appropriate amendments.

The formulas derived cover experiments even under moderate and strong fields, where few work had been done. The onset of competence of the dynamics inside the wells with the overbarrier mode would occur at fields of a few Tesla, so that comparison with experimental data would be possible. We finally remark that the treatment employed covers from the deep quantum case ($S \sim 1$) to the classical regime ($S \gg 1$). Thus, the equations derived recover, in the limit $S \rightarrow \infty$, the classical work on magnetic nanoparticles.

Acknowledgments

This work was supported by DGES, project BFM2002-00113, and DGA, project PRONANOMAG and grant no. B059/2003. We acknowledge F. Luis, L. Martín-Moreno and D. Prada for useful discussions and their support during this work.

APPENDIX A: CLASSICAL LIMIT OF BALANCE EQUATIONS

In this appendix we consider the classical limit of the balance equation (2). Any limit procedure requires to specify which quantities are kept constant and which scaled variables are needed to monitor the evolution. For the classical limit, a natural choice is to maintain fixed σ and ξ . At constant T this implies keeping the anisotropy-barrier height and amount of Zeeman energy constant. This means, that the levels tend to a continuum, so $\Delta_{m,m\pm 1} \rightarrow 0$. Then we need the behavior of $P_{m|m\pm 1}$ near $\Delta_{m,m\pm 1} = 0$. Expanding $P_{m|m'}$ up to first order, with $d_x f(x)|_{x=0} = -d_x f(-x)|_{x=0}$, and the detailed balance condition (3):

$$\left. \frac{dP_{m|m'}}{d\Delta_{m m'}} \right|_{\Delta_{m m'}=0} = -\beta \frac{1}{2} P_{m|m'}(\Delta_{m m'} = 0),$$

therefore,

$$P_{m|m'} = P_{m|m'}(0) - \frac{P_{m|m'}(0)}{2} \beta \Delta_{m m'} + \mathcal{O}(\beta \Delta_{m m'}^2) \quad (\text{A1})$$

Now, it results convenient to introduce the notation,

$$p_m \equiv P_{m+1|m}(0); \quad p_{m-1} \equiv P_{m|m-1}(0), \quad (\text{A2})$$

identifying through this appendix $\Delta_{m m'} \equiv \beta \Delta_{m m'}$ and inserting (A1) in Eq. (2),

$$\begin{aligned} \dot{N}_m &= \left(p_m + \frac{p_m}{2} \Delta_{m+1,m}\right) N_{m+1} \\ &- \left(p_m - \frac{p_m}{2} \Delta_{m+1,m}\right) N_m \\ &+ \left(p_{m-1} - \frac{p_{m-1}}{2} \Delta_{m,m-1}\right) N_{m-1} \\ &- \left(p_{m-1} + \frac{p_{m-1}}{2} \Delta_{m,m-1}\right) N_m \end{aligned} \quad (\text{A3})$$

$$\begin{aligned} \dot{N}_m &= \frac{p_m}{S^2} \left[S^2 (N_{m+1} - 2N_m + N_{m-1}) \right] \\ &+ \frac{p_m}{S^2} \left[S^2 \frac{1}{2} (\Delta_{m+1,m} N_{m+1} + \Delta_{m+1,m} N_m - \Delta_{m,m-1} N_m - \Delta_{m,m-1} N_{m-1}) \right] \\ &+ S \left(\frac{p_m}{S^2} - \frac{p_{m-1}}{S^2} \right) \left[S (N_m - N_{m-1}) + \frac{S}{2} \Delta_{m,m-1} (N_m + N_{m-1}) \right] \end{aligned} \quad (\text{A4})$$

In the first line of (A4) we recognize the usual discretization of the second derivative

$$S^2 (N_{m+1} - 2N_m + N_{m-1}) \rightarrow \frac{\partial^2 W(z, t)}{\partial z^2} \quad (\text{A5})$$

where $W(z, t)$ is the classical spin distribution. The third line can be identified with the discretizations of the first derivatives:

$$\begin{aligned} S(N_m - N_{m-1}) &\rightarrow \frac{\partial W(z, t)}{\partial z} \\ S \Delta_{m+1,m} = \beta S(\varepsilon_{m+1} - \varepsilon_m) &\rightarrow \frac{\partial u(z)}{\partial z} \\ S \left(\frac{p_{m+1}}{S^2} - \frac{p_m}{S^2} \right) &\rightarrow \frac{\partial D(z)}{\partial z} \end{aligned} \quad (\text{A6})$$

here, we have utilized that $p_m/S^2 \rightarrow D(z)$. The function $D(z)$ depends on the specific form of p_m ($\equiv P_{m+1|m}(0)$) and $u(z)$ is the classical energy function [$u(z) \equiv \beta \mathcal{H}(z)$]. Finally, the second line is the discretization of $\frac{\partial}{\partial z} \left(\frac{\partial u(z)}{\partial z} \right) W(z, t)$, since

$$\begin{aligned} S^2 \frac{1}{2} \left(\Delta_{m+1,m} N_{m+1} + \Delta_{m+1,m} N_m - \Delta_{m,m-1} N_m \right. \\ \left. - \Delta_{m,m-1} N_{m-1} \right) \rightarrow \frac{\partial}{\partial z} \left(\frac{u(z)}{\partial z} \right) W(z, t) \end{aligned} \quad (\text{A7})$$

Using (A5), (A6) and (A7), we obtain the continuum version of (2), Eq. (9), where $D(z) \equiv P_{m+1|m}(0)$

Let us emphasize that this derivation only makes use of detailed balance condition (3), and a nonvanishing transition probability at zero frequency $P_{m+1|m}(0)$, which has

where we have utilized (A2). Now, writing $p_{m-1} = p_m + [p_{m-1} - p_m]$ and multiplying the right hand side of (A3) by S^2/S^2 we obtain,

been tacitly assumed from the beginning. Considering interaction to electron-hole excitations ($F \propto S_{\pm}$), with an spectral density $J(\omega) \propto \omega$ then $D(z) \propto (1 - z^2)$ [see Eqs. (6) and (7) in Sec. II]. On the other hand, coupling to phonons (including two phonon processes) yields $D(z) \propto z^2(1 - z^2)$.

APPENDIX B: DETAILS FOR THE CALCULATION OF τ_{int} , τ_{Δ} AND τ_{ef}

Here we calculate the three time constants, τ_{int} , τ_{Δ} and τ_{ef} , which characterize the magnetization relaxation in the bimodal approximation [see Sec. IV].

(i) τ_{int}

As τ_{int} describes the low- Ω behavior of the susceptibility our purpose here is to obtain $\chi(\Omega)$ up to first order in Ω [see Eq. (17)]. For future convenience, we write N_m as,

$$N_m \cong N_m^{(0)} + N_m^{(1)} = N_m^{(0)} (1 + \beta q_m) \quad (\text{B1})$$

where $N_m^{(0)}$ and $N_m^{(1)}$ are the zero and first order (in δB_z) parts of the evolution for N_m . Inserting (B1) in (2) we obtain the set of equations necessary to calculate the response in linear approximation:

$$\begin{aligned} P_{m+1|m} - P_{m-1|m} &= i\Omega q_m + P_{m+1|m}(q_{m+1} - q_m) \\ &+ P_{m-1|m}(q_{m-1} - q_m) \end{aligned} \quad (\text{B2})$$

here $P_{m|m'} \equiv P_{m|m'}(B_z = B_z^0)$. To write (B2) in terms of $P_{m+1|m}$ and $P_{m-1|m}$ the detailed balance equation (3) and the equality $e^{\Delta_{m'm}} N_m^{(0)} = N_m^{(0)}$ have been utilized.

We are interested in the low frequency behavior, so we expand

$$q_m(\Omega) \cong q_m^{(0)} + \Omega q_m^{(1)}. \quad (\text{B3})$$

We substitute (B3) in (B2), and we solve it perturbatively in Ω . The zero-frequency order gives:

$$\begin{aligned} P_{m+1|m} - P_{m-1|m} &= P_{m+1|m}(q_{m+1}^{(0)} - q_m^{(0)}) \\ &+ P_{m-1|m}(q_{m-1}^{(0)} - q_m^{(0)}). \end{aligned} \quad (\text{B4})$$

Since (B4) depends only on the differences $q_{m+1}^{(0)} - q_m^{(0)}$, and defining

$$\bar{q}_m \equiv q_{m+1}^{(0)} - q_m^{(0)}, \quad (\text{B5})$$

equation (B4) can be casted in a two-term recurrence. With the ‘‘boundary’’ condition $P_{-S-1|-S} = 0$ the solution reads:

$$\bar{q}_m = 1 \quad (\text{B6})$$

and accordingly to (B5) and (B6),

$$q_m^{(0)} = m - M_z \quad (\text{B7})$$

where M_z is the magnetization. To obtain (B7) the normalization condition:

$$\sum_{m=-S}^S N_m^{(0)} q_m^{(0)} = 0, \quad (\text{B8})$$

has been used. The above condition comes from $\sum_m N_m^{(1)} = 0$. Besides this follows from the unicity of the Fourier expansion of the norm and $\sum_m N_m^{(0)} = 1$ plus $\sum_m N_m = 1$. Now, we write (B2) up to first order in Ω ,

$$0 = i\Omega q_m^{(0)} + P_{m+1|m}(q_{m+1}^{(1)} - q_m^{(1)}) + P_{m-1|m}(q_{m-1}^{(1)} - q_m^{(1)}). \quad (\text{B9})$$

Once more, (B4) depends only on the differences. Introducing,

$$r_m \equiv P_{m+1|m} e^{-\beta \varepsilon_m} (q_{m+1}^{(1)} - q_m^{(1)}), \quad (\text{B10})$$

equation (B9) transforms onto a two term recurrence relation, obtaining for the r_m elements,

$$r_m = -i\Omega \sum_{j=-S}^m q_j^{(0)} e^{-\beta \varepsilon_j} \quad (\text{B11})$$

where we have again invoked $P_{-S-1|-S} = 0$. Now, (B11) with (B10) and the first- Ω order normalization condition:

$$\sum_{m=-S}^S N_m^{(0)} q_m^{(1)} = 0, \quad (\text{B12})$$

permit to write $q_m^{(1)}$ as

$$iq_m^{(1)} = \sum_{i=-S}^{m-1} \frac{\Phi_i}{P_{i+1|i} N_i^{(0)}} - \sum_{j=-S}^S N_j^{(0)} \sum_{i=-s}^{j-1} \frac{\Phi_i}{P_{i+1|i} N_i^{(0)}} \quad (\text{B13})$$

where Φ_i has been defined in (26). The low- Ω expansion (17) and (B1) allows to express τ_{int} as,

$$i\tau_{\text{int}} = \frac{\beta}{\chi_z} \sum_{m=-S}^S m N_m^{(0)} q_m^{(1)}. \quad (\text{B14})$$

Introducing (B13) in (B14) and using the equalities,

$$\sum_{j=-S}^S N_j^{(0)} \sum_{i=-s}^{j-1} \frac{\Phi_i}{P_{i+1|i} N_i^{(0)}} = \sum_{i=-S}^{S-1} \frac{\Phi_i}{P_{i+1|i} N_i^{(0)}} \sum_{j=i+1}^S N_j^{(0)} \quad (\text{B15})$$

and,

$$-M_z \sum_{j=i+1}^S N_j^{(0)} + \sum_{j=i+1}^S j N_j^{(0)} = \Phi_i \quad (\text{B16})$$

we finally obtain the formula (25) for the integral relaxation time.

(ii) τ_{Δ}

The time constant τ_{Δ} arises when instead of the magnetization susceptibility, one considers the low- Ω response of the difference of the well populations Δ

$$\Delta \equiv N_+ - N_- = \sum_{m=-S}^S \text{sgn}(m - m_b) N_m, \quad (\text{B17})$$

with ε_{m_o} the maximum level. Notice that the derivation of τ_{Δ} must follow the same steps that for the derivation of τ_{int} . Further taking into account the definition of Δ and from the expression for $\chi_{\Delta}(\Omega)$ in (28) τ_{Δ} is given in terms of $q_m^{(1)}$ (B13) as:

$$i\tau_{\Delta} = \frac{1}{\chi_{\Delta}} \sum_{m=-S}^S \text{sgn}(m - m_b) N_m^{(0)} q_m^{(1)} \quad (\text{B18})$$

Finally, using equalities (B15) and

$$-\Delta \sum_{j=i+1}^S N_j^{(0)} + \sum_{j=i+1}^S \text{sgn}(m - m_b) N_j^{(0)} = \Phi_j^N, \quad (\text{B19})$$

where Φ_j^N is defined in (30), formula (29) is readily obtained.

(iii) τ_{ef}

First we notice that the definition for τ_{ef} (19) can be rewritten in terms of $N_m(t)$ as:

$$\tau_{\text{ef}}^{-1} = \frac{1}{\Delta M_z(0)} \sum_{m=-S}^S m \dot{N}_m(0). \quad (\text{B20})$$

$\dot{N}_m(0)$, is obtained directly from the balance equation making $t = 0$ in (2). Now, we recall that the system is initially at equilibrium with field $B_z = B_z^0 + \delta B_z$. Up to first order in δB_z this can be written:

$$N_m(0) = N_m^{(0)} + \delta B_z \beta N_m^{(0)} (m - M_z). \quad (\text{B21})$$

Next, we insert (B21) in (2). Considering:

$$P_{m|m\pm 1} N_{m\pm 1}^{(0)} = P_{m\pm 1|m} N_m^{(0)}, \quad (\text{B22})$$

(B20) reads:

$$\begin{aligned} \tau_{\text{ef}}^{-1} = \frac{\beta}{\chi_z} & \left(\sum_{m=-S}^S m P_{m|m-1} N_{m-1}^{(0)} \right. \\ & \left. - \sum_{m=-S}^S m P_{m+1|m} N_m^{(0)} \right) \end{aligned} \quad (\text{B23})$$

Finally, performing the change $m \rightarrow m + 1$ in the first summand we obtain the final formula (32) for the inverse of the effective time.

APPENDIX C: APPROXIMATE FORMULAS IN THE HIGH BARRIER CASE

Here we derive approximate expressions for a , Λ_1 and Λ_w in the high barrier case.

The technical difficulties deal mainly with the calculation of the sums in τ_{int} , τ_Δ and τ_{ef} . For that let us first consider the main approximation to handle with Φ_m^2 and $\Phi_m \Phi_m^N$. In the range considered Φ_m can be well approximated by:

$$\begin{aligned} \Phi_m &\cong \Phi_B; & m < S - 2 \\ \Phi_m &\cong \Phi_B + \Phi_W; & m \cong S - 1 \end{aligned} \quad (\text{C1})$$

where $\Phi_B \cong \sum_{j=-S}^{m_b} (M_z - j) N_j^{(0)} = \Phi_{m_b}$ and $\Phi_W \cong \sum_{j=m_b+1}^{S-1} (M_z - j) N_j^{(0)} = \Phi_{S-1} - \Phi_{m_b}$. Besides there are two main contributions in the sum for τ_{int} , one around m_b and the other one around $m \cong S - 1$ (see Fig. 8). This last peak in the sum is due to Φ_W . On the other hand the quantity $\Phi_m \Phi_m^N$ results well approximated for practical purposes by the constant:

$$\Phi_m \Phi_m^N \cong \Phi_B \Phi^N \quad (\text{C2})$$

with $\Phi^N = \sum_{j=-S}^{m_b} (\Delta + 1) N_j^{(0)} = \Phi_{m_b}^N$. Then the sum for τ_Δ has only one main contribution around m_b (see Fig. 8).

Now, we give the main steps to calculate the formula (34) for a . In the bimodal approximation $\tau_{\text{int}} \cong a/\Lambda_1 + (1-a)/\Lambda_w$. Then, and taking into account that $\Lambda_w \gg \Lambda_1$ and $\Lambda_1 \cong \tau_\Delta$:

$$a \cong \frac{\tau_{\text{int}}}{\tau_\Delta}. \quad (\text{C3})$$

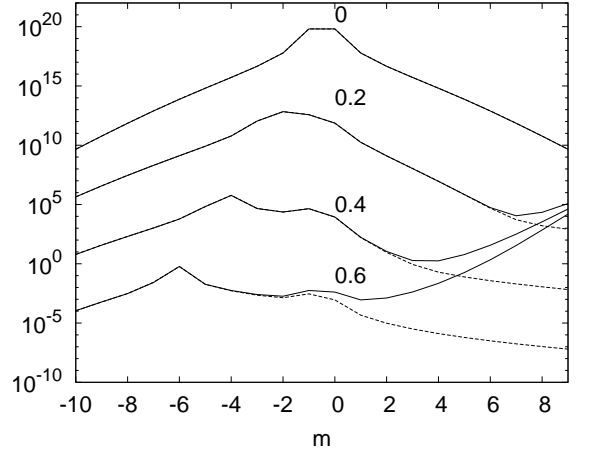


FIG. 8: Summands of τ_{int} (25), $\frac{\Phi_m^2}{N_m^{(0)} P_{m+1|m}}$, (solid line) and τ_Δ (29), $S \frac{\Phi_m \Phi_m^N}{N_m^{(0)} P_{m+1|m}}$ (dashed line). Different h are drawn: $h = 0.0, 0.2, 0.4, 0.6$. The rest of parameters are $S = 10$, $\sigma = 15$, $\lambda = 10^{-9}$.

Next we use approximations (C1) and (C2). Neglecting the second peak in the sum, which is produced by intrawell dynamics (it would contribute to the summand $(1-a)/\Lambda_w$) we write:

$$a \cong S \frac{\chi_\Delta}{\chi_z}, \quad (\text{C4})$$

here we have also used that in the high barrier limit $\Phi^B = S \Phi^N$ (see Fig. 8). Notice that (C4) depends only on equilibrium magnitudes. To compute χ_z and χ_Δ we approximate the partition function by:

$$\mathcal{Z} \cong e^\sigma \left\{ 2 \cosh \xi + e^{\sigma(q^2-1)} \cosh q\xi \right\}, \quad (\text{C5})$$

with $q = (S-1)/S$. This form for \mathcal{Z} has been calculated considering only the states $m = \pm S$ and $m = \pm(S-1)$. Restricting ourselves to the lowest states, becomes justified when $\sigma \gg 1$. However, at sufficiently high h , levels in the right well with $m < S-1$ have less energy than $m = -S+1$ even $m = -S$, then they would be more populated. On the other hand, this is the minimal model which includes sufficient states to deal with intrawell and overbarrier contributions. Then, from (C5) we obtain χ_z and χ_Δ . Finally, considering only the leading terms in σ we obtain the final expression (34) for a .

Now we turn our attention to Λ_1 . In the main text we have argued that $\Lambda_1 \cong \tau_\Delta^{-1}$. Then, and considering (C2), we write:

$$\Lambda_1^{-1} \cong \tau_\Delta \cong \frac{\beta}{\chi_\Delta} \Phi \Phi^N \sum_{m=-S}^{S-1} \frac{1}{N_m^{(0)} P_{m+1|m}}. \quad (\text{C6})$$

We use now θ_m [see Eq. (27)], i.e. $\theta_m = \sum_{j=m+1}^S N_j^{(0)}$; then it can be checked that:

$$\Delta \cong 2\theta_{m_b} - 1 \quad (\text{C7})$$

and

$$\chi_{\Delta} \cong 2\partial_{B_z}\theta_{m_b} = 2\beta\Phi^B \quad (\text{C8})$$

Thus Λ_1^{-1} reads:

$$\Lambda_1^{-1} \cong (1 - \theta_{m_b})\theta_{m_b} \sum_{m=-S}^{S-1} \frac{1}{N_m^{(0)} P_{m+1|m}}. \quad (\text{C9})$$

First, Eq. (C9) equals the Würger result (27), since $\theta_m \cong \theta_{m_b} = 1/2$. Furthermore, the sums for θ_{m_b} and $\sum 1/N_m^{(0)} P_{m+1|m}$ can be evaluated following Garanin in some limiting cases [16]. In particular the classical limit can be carried out. In this limit the sum is converted into an integral, which in turn can be solved. Then using approximate expressions for the classical \mathcal{Z} when $\sigma \gg 1$ (see Sec. II of [29]) and the same for θ_{m_b} , we recover the Brown result (31) for $D(z) \propto (1 - z^2)$ [see Eq. (9)]. Eventually, one also considers $\sigma/S > 1$ to evaluate the sums in (C9). In this case, becomes sufficient consider only the two main terms in the sum, namely $1/N_m^{(0)} P_{m_b+1|m_b}$ and $1/N_m^{(0)} P_{m_b-1|m_b}$. In addition we only take into account the leading terms in σ for θ_{m_b} , obtaining the Arrhenius formula (35) for Λ_1 .

Finally we consider Λ_w . In the expression for Λ_w [Eq.(23)], the denominator can be approximated by $\Lambda_1 \tau_{\text{int}}^{-1} - 1 \cong a - 1$ [see Eq. (C3)]. Finally assuming $\tau_{\text{ef}}^{-1} \gg \Lambda_1$ (see Fig. 4) Λ_w reads:

$$\Lambda_w \cong \frac{\tau_{\text{ef}}^{-1}}{1 - a} \quad (\text{C10})$$

Then Λ_w/Λ_1 :

$$\frac{\Lambda_w}{\Lambda_1} = \frac{1}{4S^2} \frac{a}{1 - a} \left(\sum_{m=-S}^{S-1} N_m^{(0)} P_{m+1|m} \right) \times \left(\sum_{m=-S}^{S-1} \frac{1}{N_m^{(0)} P_{m+1|m}} \right). \quad (\text{C11})$$

To obtain this formula we have used equation (C6) for Λ_1 and (C4) for a together with $\Phi_B \cong S\Phi^N$. Now, taking only leading terms in the sum we readily obtain (36) in the regime of interest.

APPENDIX D: EXACT ANALYTICAL SUSCEPTIBILITY FOR S=1

When $S = 1$ it is possible to derive an exact analytical expression for $\chi(\Omega)$. For that, we calculate the eigenvalues of the, in this case, 3×3 relaxation matrix \mathcal{R} , obtaining:

$$\Lambda_{1,2} = (\Gamma_+ + \Gamma_-) \mp \sqrt{(\Gamma_+ - \Gamma_-)^2 + 4P_{1|0}^{(0)} P_{-1|0}^{(0)}}, \quad (\text{D1})$$

plus the zero eigenvalue, $\Lambda_0 = 0$. Here $\Gamma_{\pm} \equiv P_{\pm 1|0}[1 + \exp\{\beta(\epsilon_{\pm 1} - \epsilon_0)\}]$. Notice that the bimodal description is exact for $S = 1$ since $\Lambda_w \equiv \Lambda_2$. Besides, using the relation of τ_{ef}^{-1} with the eigenvalues, *i.e.* $\tau_{\text{ef}}^{-1} = a\Lambda_1 + (1 - a)\Lambda_2$ [Eq.(24)] a yields:

$$a = \frac{1}{\Lambda_2 - \Lambda_1} (\Lambda_2 - \tau_{\text{ef}}^{-1}), \quad (\text{D2})$$

with $\tau_{\text{ef}}^{-1} = \beta/(\chi_z \mathcal{Z})(P_{1|0}^{(0)} + P_{-1|0}^{(0)})$.

The two modes Λ_1 , Λ_2 and a are introduced in (16) obtaining the exact expression for the response.

-
- [1] Q. A. Pankhurst and R. J. Pollard, J. Phys.: Condens. Matter **5**, 8487 (1993).
 - [2] L. Néel, Ann. Geophys. **5**, 99 (1949).
 - [3] W. F. Brown, Jr., Phys. Rev. **130**, 1677 (1963).
 - [4] S. J. Blundell and F. L. Pratt, J. Phys.: Condens. Matter **16**, R771 (2004).
 - [5] P. Hänggi, P. Talkner, and M. Borkovec, Rev. Mod. Phys. **62**, 251 (1990).
 - [6] V. I. Mel'nikov, Phys. Rep. **209**, 1 (1991).
 - [7] W. T. Coffey, D. Crothers, Y. P. Kalmykov, and J. T. Waldrom, Phys. Rev. B **51**, 15947 (1995).
 - [8] D. A. Garanin, Phys. Rev. E **54**, 3250 (1996).
 - [9] Y. P. Kalmykov, W. T. Coffey, and S. V. Titov, J. Magn. Mag. Mater. **265**, 44 (2003).
 - [10] D. A. Garanin and E. M. Chudnovsky, Phys. Rev. B **56**, 11 102 (1997).
 - [11] F. Luis, J. Bartolomé, and J. F. Fernández, Phys. Rev. B **57**, 505 (1998).
 - [12] F. Hartmann-Boutron, P. Politi, and J. Villain, Int. J. Mod. Phys. B **10**, 2577 (1996).
 - [13] A. Würger, J. Phys.: Condens. Matter **10**, 10075 (1998).
 - [14] J. Villain, F. Hartmann-Boutron, R. Sessoli, and A. Rettori, Europhys. Lett. **27**, 159 (1994).
 - [15] A. Würger, Phys. Rev. Lett. **81**, 212 (1998).
 - [16] D. A. Garanin, Phys. Rev. E **55**, 2569 (1997).
 - [17] Y. P. Kalmykov, W. T. Coffey, and S. V. Titov, Phys. Rev. E **69**, 021105 (2004).
 - [18] The maximum level is given by $m_b = -B_z/2D + F$, with $F = \mathcal{F}[B_z/2D + S + 1/2] - 1/2$ and $\mathcal{F}[x]$, the fractional part of x .
 - [19] J. L. García-Palacios and D. Zueco (2005), submitted to J. Phys. A, quant-ph/05.

- [20] H. M. Cataldo, *Physica A* **165**, 249 (1990).
- [21] S. Dattagupta, *Relaxation phenomena in condensed matter physics* (Academic, Orlando, 1987).
- [22] E. Anderson, Z. Bai, C. Bischof, J. Demmel, J. Dongarra, J. D. Croz, A. Greenbaum, S. Hammarling, Z. MckKenney, S. Ostrouchov, et al., *LAPACK User's guide* (SIAM, Philadelphia, 1995), <http://www.netlib.org/lapack/>.
- [23] For S half-integer, at $h = 0$ the $(2S + 1)$ states are double degenerated: $|\Lambda_0\rangle = |\Lambda_1\rangle = 0$ ($P_{-1/2|1/2} = 0$). The rest of eigenvalues describe symmetrical processes in both wells analogous to the ones explained for S integer.
- [24] A. Aharoni, *Phys. Rev.* **177**, 793 (1969).
- [25] W. T. Coffey, P. J. Cregg, and Y. P. Kalmykov, *Adv. Chem. Phys.* **83**, 263 (1993).
- [26] At $h = (2n + 1)/(2S - 1)$ the lowest eigenvalue goes to zero. At these bias $m = -n$ and $m = -n + 1$ becomes degenerate, thus the relaxation time diverges, since $P_{-n|-n+1}(0) = 0$ in the model used.
- [27] D. A. Garanin, *Europhys. Lett.* **48**, 486 (1999).
- [28] M. N. Leuenberger and D. Loss, *Phys. Rev. B* **61**, 1286 (2000).
- [29] J. L. García-Palacios, *Adv. Chem. Phys.* **112**, 1 (2000).